East European Journal of Physics. 3. 192-197 (2023)
DOI:10.26565/2312-4334-2023-3-16 ISSN 2312-4334

THE INFLUENCE CHANGING OF NUCLEAR POTENTIAL ON QUASI-ELASTIC SCATTERING IN $^{16}O+^{160}Gd$ AND $^{12}C+^{197}Au$ SYSTEMS[†]

Farah J. Hamood[§], Khalid S. Jassim*
Department of Physics, College of Education for pure Sciences, University of Babylon, Iraq
**Corresponding Author e-mail: khalidsj@uobabylon.edu.iq, [§]e-mail: pure.farah.jabar@uobabylon.edu.iq*
Received March 12, 2023; revised May 3, 2023; accepted May 5, 2023

In this research, the effect of changing the potential depth V_0 on the Quasi-elastic scattering and barrier distribution calculations have been studied using Wood-Saxon (WS) potential for $^{16}O+^{160}Gd$ and $^{12}C+^{197}Au$ systems. The chi square ($\chi 2$) is applied to compare the best fitted value of the diffuseness parameter between the theoretical calculations and the experimental data. The diffuseness parameter which used in this work is to be at standard value 0.63. The χ^2 was applied to most suitable the better fitted value of the potential depth V_0. According to the results, we noticed that some systems achieved a good match between the theoretical calculations and experimental data of Quasi-elastic scattering ($d\sigma qel/d\sigma R$) and the distribution calculations at the standard value of the potential depth or at a value lower than the standard value and no match was achieved at a value greater than the standard value of the potential depth V_0. We conclude that the values of quasi-elastic scattering values increase when the value of potential depth decreases.
Keywords: *Quasi-elastic scattering; Woods-Saxon (WS) potential; Coupled; Heavy-ion system; Surface diffuseness parameter*
PACS: 21.60.-n, 21.10.-k, 21.60.Jz, 25.70.Bc, 25.70.

1. INTRODUCTION

The potential between two nuclei interaction, which comprises the short-range attractive and absorptive nuclear potentials as well as the long-range Coulomb potential, has always been a fundamental topic in nuclear physics. The Coulomb contact between two nuclei is widely understood, but describing the nuclear component is significantly more complex. Over the last few decades, the optical model potential (OMP) has been widely used to characterize the nuclear component, and numerous alternative potential forms have been proposed to replicate a large amount of nuclear reaction data [1][2]. In addition to nuclear reactions driven by light particles, the optical system may also be involved in nuclear reactions between heavy ions. The nuclear potential is often assumed to be of Woods-Saxon type, with three parameters defining it: depth, radius, and diffuseness. The diffuseness parameter defines the nuclear potential's fall-off and hence has a direct impact on the barrier width and coupling strengths, which are first order dependent on the derivative of the potential [3][4][5]. Quasi-elastic scattering is defined as "the sum of elastic scattering, inelastic scattering, and transfer reaction [6][7]. Quasi-elastic scattering is similar to the fusion process [7], which is defined as the combination of two different nuclei to generate a composite system. The Negative of the first derivative of the ratio of quasi-elastic to Rutherford cross-section, dqel/dR, with regard to the energy E, or D_{qel} = d(dqel/dR)/dE, is used to determine the quasi-elastic barrier distribution [8]. Several studies on quasi elastic scattering have been studied by Khalid S. Jassim for some heavy ions systems [9]–[11]. They demonstrated the nucleus-nucleus potential for several heavy ions by a comprehensive investigation of the surface characteristics. The nuclear potential has been described using WS, single-channel SC, and coupled-channel CC calculations, which were between the relative motion of colliding nuclei and their intrinsic motions, and they discovered that the best fitted value of the diffuseness parameter was obtained through a coupled-channel calculation with an inert target and excited projectile for the current work.

The aims of the present work is to study the influence changing of nuclear potential (potential depth V_0) on quasi-elastic scattering in systems $^{16}O+^{160}Gd$, $^{12}C+^{197}Au$ at surface diffuseness parameter it determined in earlier by the method chi square, we used The CQEL program [12] which contains all orders of coupling and is the most current iteration of the computer code CCFULL, was used to calculate single and coupled channels.

2. THEORY

The nucleus-nucleus potential is made up of two components, the first of which is the nuclear potential V_n, which may be properly and appropriately described by the other two parts of the potential between two nuclei. The form for Woods-Saxon (WS) supplied by [13]:

$$V_N(r) = -\frac{V_\circ}{1+e^{[\frac{r-R_\circ}{a}]}}, \quad (1)$$

where r represents the distance between the projectile's mass number AP and the target's mass number A_T at the center of mass, and R_0 stands for the system's radius: $R_0 = r_0\left(A_T^{\frac{1}{3}} + A_P^{\frac{1}{3}}\right)$. The second portion, which represents the Coulomb

[†] ***Cite as:*** F.J. Hamood, K.S. Jassim, East Eur. J. Phys. 3, 192 (2023), https://doi.org/10.26565/2312-4334-2023-3-16

potential V_C between two spherical nuclei with uniform charge density distributions when they are not interacting, is given by[13]:

$$V_c(r) = \frac{Z_P Z_T \ e^2}{r}, \tag{2}$$

where r is the distance between the centers of mass of the colliding nuclei, Z_p and Z_T are the atomic numbers of projectile and target, respectively. The Coulomb potential is produced when the nuclei interact, and it is determined by [14]:

$$V_c(r) = \frac{Z_P Z_T \ e^2}{2R_C}\left[3 - \left(\frac{r}{R_c}\right)^2\right], \tag{3}$$

where the projectile and target nuclei are represented by spheres of radii R_c. Two nuclei collide as a result of the nuclear intrinsic motion and the relative motion of their centers of mass, r = (r, r). The following is the Hamiltonian system[15]:

$$H(\vec{r}.\xi) = -\frac{\hbar^2}{2\mu}\nabla^2 + V(r) + H_0(\xi) + V_{coup}(\vec{r}.\xi), \tag{4}$$

where *V(r)* is the bare potential in the absence of coupling where $V(r) = V_N(r)+V_c(r)$, $H_0(\xi)$ is the Hamiltonian for the intrinsic motion, and V_{coup} is the stated coupling r stands for the center of mass distance between the colliding nuclei. The Schrodinger equation to wave functions is given by[16]:

$$(-\frac{\hbar^2}{2\mu}\nabla^2 + V(r) + H_0(\xi) + V_{coup}(\vec{r}.\xi))\psi(\vec{r}.\xi) = E\psi(\vec{r}.\xi), \tag{5}$$

Internal degrees of freedom have a limited spin in general. the coupling Hamiltonian may be expressed as [15]:

$$V_{coup}(\vec{r}.\xi) = \sum_{\lambda>0.\mu} f_\lambda\ (r)Y_{\lambda\mu}(\hat{r}).T_{\lambda\mu}(\xi), \tag{6}$$

The internal coordinate is used to create the harmonics and spherical tensors, which are represented by the notations $Y_{\lambda\mu}(\hat{r})$ and $T_{\lambda\mu}(\xi)$, respectively. That when it was considered in V(r), the sum of all values of excluding for λ(r) = 0. For a constant total angular momentum J and its z-component M, the expansion basis for the wave function in Eq. (5) is given by [15]:

$$\langle \vec{r}\,\xi|(nlI)JM\rangle = \sum_{m_1 m_I}\langle lm_l\, Im_I|JM\rangle Y_{lm_l}(\hat{r})\,\varphi_{nIm_I}(\xi), \tag{7}$$

where *l* stands for the orbital, *I* – internal angular momenta, and $\varphi_{nIm_I}(\xi)$ the wave function for the internal motion that is give by the equation below[15] .

$$H_0(\xi)\,\varphi_{nIm_I}(\xi) = \epsilon_n\,\varphi_{nIm_I}(\xi)\,, \tag{8}$$

The total wave function $\psi(\vec{r}.\xi)$has been expanded as[16]:

$$\psi(\vec{r}.\xi) = \sum_{n.l.I}\frac{u^J_{nlI}(r)}{r}\langle \vec{r}\,\xi|(nlI)JM\rangle, \tag{9}$$

The Schrödinger equation [Eq. (3)] can be written as a collection of linked equations for $u^J_{nlI}(r)$:[16]

$$\left[-\frac{\hbar^2}{2\mu}\frac{d^2}{dr^2} + V(r) + \frac{l(l+1)\hbar^2}{2\mu r^2} - E + \epsilon_n\right]u^J_{nlI}(r) + \sum_{ń.l'.Í}V^J_{nlJ;ń.l'.Í}(r)u^J_{ń.l'.Í}(r) = 0 \tag{10}$$

The coupling matrix elements$V^J_{nlJ;ń.\,l'.Í}(r)$, According to [15] are as follows:

$$V^J_{nlJ;ń.Í.Í}(r) = \langle JM\ (nlI)\left|V_{coup}(\vec{r}.\xi)\right|\left(ń.l'.Í\right)JM\rangle = \sum_\lambda(-1)^{I-Í+l'+J}f_\lambda(r)\langle l||Y_\lambda||l'\rangle\langle nI||T_\lambda||n'I'\rangle \times \sqrt{(2l+1)(2I+1)}\begin{Bmatrix} I' & l' & J \\ l & I & \lambda\end{Bmatrix}, \tag{11}$$

Where the reduced matrix elements in Eq. (8) is defined as follows[15]:

$$\langle l_{ml}|Y_{\lambda\mu}|l'_{ml'}\rangle = \langle l'_{ml'}\,\lambda\mu|l_{ml}\rangle\langle l||Y_\lambda||l'\rangle, \tag{12}$$

where $V^J_{nlJ;ń.\,l'.Í}(r)$ are separate of the index M, the index has been suppressed as seen in Eq (11). Coupled-channels equations are the name given to the equation (10). For heavy-ion fusion reactions, these equations are usually solved using the incoming wave boundary conditions[16].

$$u^J_{nlI}(r) \sim \mathcal{I}^J_{nlI}\ exp\left(-1\int_{r_{abs}}^{r}k_{nlI}\,(ŕ)dŕ\right)\ .r \leqslant r_{abs} \tag{13}$$

$$\frac{i}{2}\left(H_l^{(-)}\,(k_{nIr})\delta_{n,n_i}\delta_{l,l_i}\delta_{I,I_i} + \sqrt{\frac{k_{nIi}}{k_{nI}}}\,S^J_{lI}H_l^{(+)}(k_{nIr})\right)\ ,\ r \longrightarrow \infty\,, \tag{14}$$

where $k_{nIr} = \sqrt{2\mu(E-\epsilon_{nI})/\hbar^2}$, $k_{nIi} = k = \sqrt{2\mu E/\hbar^2}$ and the following formula defines the local wave number k_{nII}:

$$k_{nII}(r) = \sqrt{\frac{2\mu}{\hbar^2}\left(E - \epsilon_{nI} - \frac{l(l+1)\hbar^2}{2\mu r^2} - V(r) - V^J_{nlJ;nlJ}(r)\right)} \quad (15)$$

Following the determination of the transmission coefficients Tn_{lIJ}, the penetrability through the Coulomb barrier is provided by:

$$P^J_{liIi}(E) = \sum_{n.l.I} \frac{k_{nII}(r_{abs})}{k} |\mathcal{T}^J_{nlI}|^2 \quad (16)$$

In contrast to the computation of fusion cross sections, the computation of quasi-elastic cross sections often requires a large value of angular momentum in order to yield convergent results. The potential pocket at ($r = r_{abs}$) grows shallow or even disappears for such a large angular momentum. The incoming flux in Eq (13) cannot, however, be clearly identified. The quasi-elastic problem frequently uses the regular boundary conditions at the origin in order to avoid using the incoming wave boundary conditions. When using the standard boundary conditions, a complex potential VN(r) = VN0(r)+iw(r) is needed to simulate the fusion reaction. After obtaining the nuclear S-matrix in Equation (Eq11). The scattering amplitude may be calculated using

$$f^J_{ll}(\theta.E) = i\sum_{Jl}\sqrt{\frac{\pi}{kk_{nI}}} i^{J-l}\, e^{i[\sigma_J(E)+\sigma_l(E-\epsilon_{nI})]}\sqrt{2J+1}\, Y_{l0}(\theta)\left(S^J_u - \delta_{I.I_2}\delta_{l.l_2}\right) + f_c(\theta.E)\delta_{I.I_2}\delta_{l.l_2} \quad (17)$$

The Coulomb phase shift is σ_l.and given by the equation,

$$\sigma_l = |\Gamma(l+1+i\eta)|, \quad (18)$$

As for f_c, which is the Coulomb scattering amplitude and is determined by[16]:

$$f_c(\theta.E) = \frac{\eta}{2ksin^2\left(\frac{\theta}{2}\right)} e^{\left[-i\eta ln\left(sin^2\left(\frac{\theta}{2}\right)\right)+2i\sigma_0(E)\right]}, \quad (19)$$

where η is the Somerfield parameter which is given by $\eta = Z_1 Z_2\, e^2/\hbar v$, and utilizing Equation (16), the differential cross section may be evaluated

$$\frac{d\sigma_{qel}(\theta.E)}{d\Omega} = \sum_{Jll} \frac{k_{nI}}{k} |f^J_{ll}(\theta.E)|^2, \quad (20)$$

May be evaluate the Rutherford cross section.

$$\frac{d\sigma_R(\theta.E)}{d\Omega} = |f_c(\theta.E)|^2 = \frac{\eta^2}{4k^2}\frac{1}{\sin^4\left(\frac{\theta}{2}\right)}, \quad (21)$$

The distribution of the barrier of fusion is defined as [15]:

$$D_{fus}(E) = \frac{d^2}{dE^2}\left[E\ \sigma_{fus}(E)\right], \quad (22)$$

The definition of the total scattering distribution of the barrier of scattering $D_{tot}(E)$ is[15].

$$D_{tot}(E) = -\frac{d}{dE}\left[\frac{d\sigma_{tot}}{d\sigma_R}(E)\right], \quad (23)$$

3. RESULTS AND DISCUSSION

The single-channel and coupled-channel computations were performed with the CQEL program, which is the most recent edition of the computer code CCFULL[12]. To eliminate systematic errors in the current study, the chi square technique χ^2 was used as a normalizing factor between the theoretical calculation and the experimental data. These computations were performed using a WS form for the nuclear potential, which has real and imaginary components. The imagined potential was utilized to explain the relatively low internal absorption following barrier penetration. The parameters of the actual potential were investigated in order to obtain the best fit to the experimental data, which was then replicated for all interactions.

3.1 $^{16}O+^{160}Gd$ System

In this reaction were processed in two cases, the first case, where both the projectile and target nuclei were considered inert (SC) at three values of the real nuclear potential (potential depth V_0) (58.7, 83.7 and 108.7) MeV and we considered the diffusion parameter 0.50 fm. It was previously determined by χ^2 method as the best value for matching the experimental data with the theoretical data. In the second case, the target core ^{160}Gd was rotation this was deduced according to the ratio $E_{4^+}/E_{2^+} = 3.3$ with a deformation coefficient of β_2=0.280 and β_2= 0.065. We used the single-quadrupole and third-octupole phonon excitation to the state 2^+ (0.075263 MeV), at coupled-channel (CC). While the projectile nucleus was ^{16}O vibration where E_{4^+}/E_{2^+} =1.49 with a deformation coefficient of β_2 = 0.364 with single-quadrupole phonon excitation to the state 2^+ (6.9171 MeV) and the radius parameter r_0=1.2 fm

Table 1. The values of the **WS** potential's parameters and χ^2 fitting between experimental and theoretical data for the **^{16}O+^{160}Gd reaction**.

System	Channel	a_0 (fm)	r_0 (fm)	V_0 (MeV)	θ_{cm} $(deg.)$	χ^2	
						σ_{qel}/σ_R	D_{qel}
^{16}O+^{160}Gd	SC	0.50	1.2	58.7	170	0.04873	0.0072179
				83.7		0.12627	0.0055259
				108.7		0.27427	0.0074302
	CC	0.50	1.2	58.7	170	0.00522	0.0034521
				83.7		0.01035	0.0034493
				108.7		0.02409	0.0057510

By the comparing between the experimental data and the theoretical calculations, we shown that in Table (1), we notice that the better value for the quasi-elastic scattering $(\frac{d\sigma_{qel}}{d\sigma_R})$ = 0.04873 at the depth potential V_0 = 58.7MeV, which was acquired from SC data analysis where the projectile ^{16}O nucleus and target ^{16}Gd nucleus are inert. It was shown by the hard red line in Fig. 1a. (A). This is the curve that is nearest to the curve of the experimental data. The batter value for the distribution D = 0.0055259 at the depth potential V_0 = 83.7 MeV. According to the coupled-channel calculation with a rotating target (T) and vibrating projectile (P), the best value of $(\frac{d\sigma_{qel}}{d\sigma_R})$ = 0.00522 at the depth potential V_0 = 58.7 MeV, was shown by the hard red line in Fig. 1.b (B) We note from the draw It is the curve nearest to the curve of the experimental result, while the best value to the distribution D = 0.0034493 at the depth potential V_0=83.7 represented by the green colored curve.

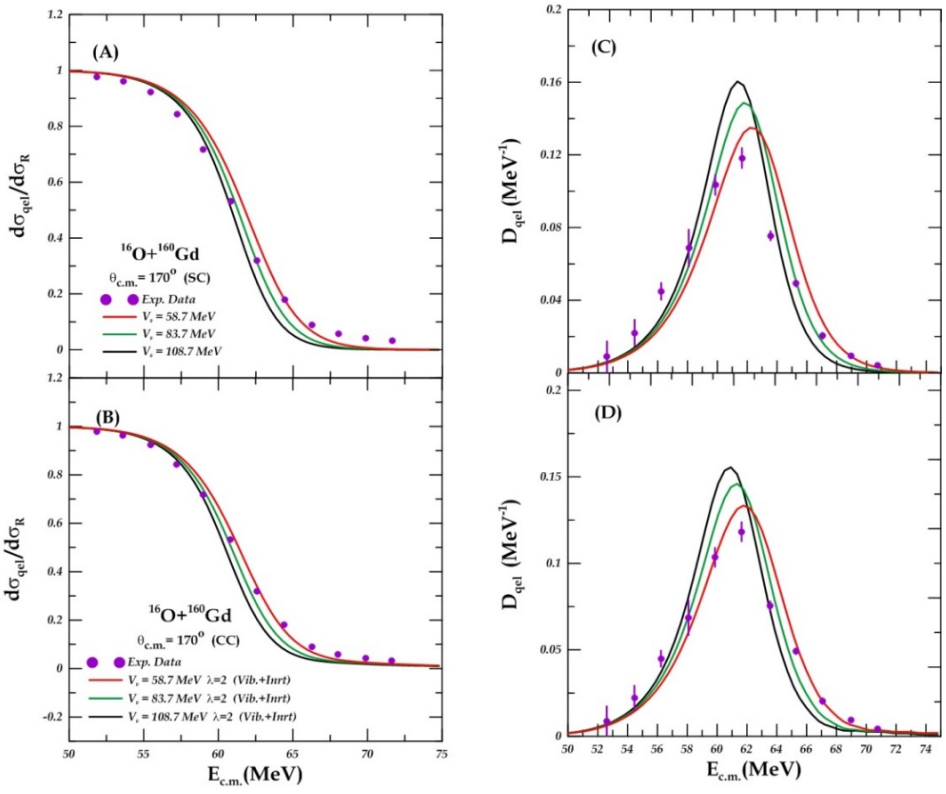

(a) (b)

Figure 1a. The ratio of the quasi-elastic scattering to the Rutherford cross sections for ^{16}O+^{160}Gd system at sub-barrier energies. Banal A and B using the single channel and coupled-channels calculations, respectively. **Figure 1.b.** (C, D) shows the distribution at sub-barrier energies, using the single and coupled channels calculations, respectively.

3.2 ^{12}C+^{197}Au system

In this reaction, the results were split into two stages. In the first stage, according to single channel (SC) calculations, the projectile and target nuclei were inert at various real nuclear potentials (potential depth V_0) (48.8, 58.8, and 68.8) MeV, and the diffusion parameter was 0.63 fm, which had previously been determined by the chi-square χ^2 method to be the nearest value between the experimental and theoretical data. In the second stage, at coupled-channel (CC) calculations, the projectile nucleus **^{12}C** was rotation where E_{4^+}/E_{2^+}= 2.9 with a deformation coefficient of β_2 = 0.582 with single quadrupole phonon excitation to the state 2^+ (4.43982 MeV). The target nucleus was **^{197}Au**. In the rotation state, this was deduced according to the ratio $E_{5/2^+}/E_{1/2^+}$ = 3.6 with a deformation coefficient of β_2 =-0.131, β_4= - 0.031. We excited the state 2^+ (0.077351 MeV) with single-quadrupole and third-octupole phonons. The radius parameter r_0 is equal to 1.2 fm.

Table 2. The values of the **WS** potential's parameters and χ^2 fitting between experimental and theoretical data for the $^{12}C+^{197}Au$ reaction.

System	Channel	a_0 (fm)	r_0 (fm)	V_0 (MeV)	θ_{cm} $(deg.)$	χ^2	
						σ_{qel}/σ_R	D_{qel}
$^{12}C+^{197}Au$	SC	0.63	1.2	48.8	180	0.0508598	0.0099349
				58.8		0.1054816	0.0149919
				68.8		0.2342481	0.0349948
	CC	0.63	1.2	48.8	180	0.0133151	0.0230850
				58.8		0.0059362	0.0350599
				68.8		0.0063233	0.0522743

The comparing between the experimental data and the theoretical calculations show in Table (2), from this table, We notice that the best value for the quasi-elastic scattering $(\frac{d\sigma_{qel}}{d\sigma_R})$ = 0.0508598 at the depth potential V_0 = 48.8MeV, which was obtained from SC data analyses when the projectile ^{16}O nucleus and target ^{197}Au nucleus are inert and it was represented by the hard red line in Fig.2.a (A). This is the curve that is closest to the experimental data curve. The batter value for the distribution D = 0.0099349 at the same depth potential V_0. Then, by using the coupled-channel accounts with a rotating target (T) and vibrating projectile (P), the better value of the quasi-elastic scattering $(\frac{d\sigma_{qel}}{d\sigma_R})$ = 0.0059362 at the depth potential V_0 = 58.8 MeV. It was represented by the hard green line in Fig. 2.b (B) as the figure shows. It is the curve closest to the experimental data curve, with the best value for the distribution D = 0.0230850 at the depth potential V_0 = 48.8 MeV represented by the red colored curve.

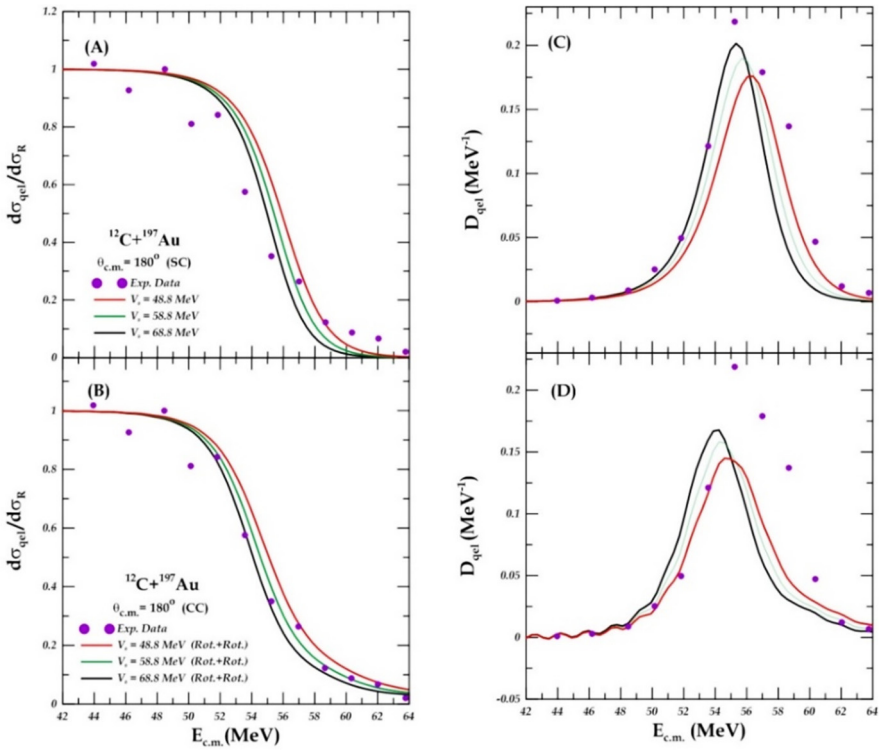

(a) (b)

Figure 2.a. The ratio of the quasi-elastic scattering to the Rutherford cross sections for $^{12}C+^{197}Au$ system at sub-barrier energies. Banal A and B using the single channel and coupled-channels calculations, respectively. **Figure 2.b.** (C, D) shows the distribution at sub-barrier energies, using the single and coupled channels calculations, respectively. The experimental data are taken from Ref. [17].

4. CONCLUSIONS

In this research we concluded the following:

1- When the value of the potential depth decreases, it leads to a decrease in the value of the nuclear potential, and thus the height of the potential barrier will increase, the Quasi-elastic scattering calculations will increase, and the potential barrier distribution curve will shift to the right.

2- When the potential depth increases, the nuclear potential also increases, so the potential barrier will decrease and lead to a decrease in semi-elastic scattering calculations and a decrease in the height of the potential barrier distribution and its shift to the left.

ORCID ID

Khalid S. Jassim, https://orcid.org/0000-0002-5990-3277

REFERENCES

[1] M.Y.H. Farag, E.H. Esmael, and H.M. Maridi, "Analysis of proton-Be 9, 10, 11, 12 scattering using an energy-, density-, and isospin-dependent microscopic optical potential," Phys. Rev. C, **90**(3), 034615 (2014). https://doi.org/10.1103/PhysRevC.90.034615

[2] C.J. Lin, H.M. Jia, H.Q. Zhang, F. Yang, X.X. Xu, F. Jia, Z.H. Liu, and K. Hagino, "Systematic study of the surface properties of the nuclear potential with high precision large-angle quasi-elastic scatterings," Phys. Rev. C, **79**(6), 064603 (2009). https://doi.org/10.1103/PhysRevC.79.064603

[3] N.T. Zhang, Y.D. Fang, P.R.S. Gomes, J. Lubian, M.L. Liu, X.H. Zhou, G.S. Li, *et al.*, "Complete and incomplete fusion in the ^{9}Be + ^{181}Ta reaction," Phys. Rev. C, **90**(2), 024621 (2014). https://doi.org/10.1103/PhysRevC.90.024621

[4] V. Avrigeanu, and M. Avrigeanu, "Consistent optical potential for incident and emitted low-energy α particles," Phys. Rev. C, **91**(6), 064611 (2015). https://doi.org/10.1103/PhysRevC.91.064611

[5] T. Furumoto, Y. Sakuragi, and Y. Yamamoto, "Dynamical evolution of heavy-ion scattering in the high-energy region," Prog. Theor. Phys. Suppl. **196**, 219-224 (2012). https://doi.org/10.1143/PTPS.196.219

[6] K. Hagino, "Recent developments in quasi-elastic scattering around the Coulomb barrier," AIP conference proceedings, **891**(1), 80-88 (2007). https://doi.org/10.1063/1.2713503

[7] K. Washiyama, K. Hagino, and M. Dasgupta, "Probing surface diffuseness of nucleus-nucleus potential with quasielastic scattering at deep sub-barrier energies," Phys. Rev. C, **73**(3), 034607 (2006). https://doi.org/10.1103/PhysRevC.73.034607

[8] M. Beckerman, "Subbarrier fusion of atomic nuclei," Phys. Rep. **129**(3), 145-223 (1985). https://doi.org/10.1016/0370-1573(85)90058-4

[9] A.J. Hassan, and K.S. Jassim, "Effect of Surface Diffuseness Parameter on Quasi-elastic Scattering Calculations for ^{6}He+^{64}Zn, ^{7}Li+^{64}Zn and ^{8}Li+^{90}Zr Systems," NeuroQuantology, **18**(9), 40 (2020). https://doi.org/10.14704/nq.2020.18.9.NQ20214

[10] N.H. Hayef, and K.S. Jassim, "Coupled channels for quasi-elastic scattering of determining diffuseness parameters in Woods-Saxon potential for nuclear reaction," in AIP Conference Proceedings, **2414**(1), 030012 (2023). https://doi.org/10.1063/5.0117002

[11] Q.J. Tarbool, K.S. Jassim, and A.A. Abojassim, "Surface diffuseness parameter with quasi-elastic scattering for some heavy-ion systems," Int. J. Nucl. Energy Sci. Technol. **13**(2), 110-119 (2019). https://www.inderscienceonline.com/doi/abs/10.1504/IJNEST.2019.100758

[12] K. Hagino, N. Rowley, and A. T. Kruppa, "A program for coupled-channel calculations with all order couplings for heavy-ion fusion reactions," Comput. Phys. Commun. **123**(1-3), 143-152 (1999). https://doi.org/10.1016/S0010-4655(99)00243-X

[13] R.D. Woods, and D.S. Saxon, "Diffuse surface optical model for nucleon-nuclei scattering," Phys. Rev. **95**(2), 577 (1954). https://doi.org/10.1103/PhysRev.95.577

[14] P. Fröbrich, and R. Lipperheide, *Theory of nuclear reactions*(*Oxford Studies in Nuclear Physics*), vol. 18, 1st ed. (Oxford university Press. Inc., New York, 1996).

[15] K. Hagino, and N. Rowley, "Large-angle scattering and quasielastic barrier distributions," Phys. Rev. C, **69**(5), 054610 (2004). https://doi.org/10.1103/PhysRevC.69.054610

[16] M. Dasgupta, D.J. Hinde, J.O. Newton, and K. Hagino, "The nuclear potential in heavy-ion fusion," Prog. Theor. Phys. Suppl. **154**, 209-216 (2004). https://doi.org/10.1143/PTPS.154.209

[17] M.B. Tsang, *et al.*, "Azimuthal correlations between light particles emitted in ^{12}O induced reactions on ^{12}C and ^{197}Au at 400 MeV," Phys. Lett. B, **148**(4-5), 265-269 (1984). https://doi.org/10.1016/0370-2693(84)90085-6

ВПЛИВ ЗМІНИ ЯДЕРНОГО ПОТЕНЦІАЛУ НА КВАЗІПРУЖНЕ РОЗСІЮВАННЯ В СИСТЕМАХ ^{16}O+^{160}Gd ТА ^{12}C+^{197}Au

Фарах Дж. Хамуд, Халід С. Джасім

Факультет фізики, Освітній коледж чистих наук, Вавилонський університет, Ірак

У цьому дослідженні було вивчено вплив зміни глибини потенціалу V_0 на квазіпружне розсіювання та розрахунки розподілу бар'єрів за допомогою потенціалу Вуда-Саксона (WS) для систем ^{16}O+^{160}Gd і ^{12}C+^{197}Au. Хі-квадрат ($\chi 2$) використовується для порівняння найкраще підігнаного значення параметра дифузності між теоретичними розрахунками та експериментальними даними. Параметр дифузності, який використовується в цій роботі, повинен мати стандартне значення 0,63. $\chi 2$ було застосовано до найбільш підходящого, краще підігнаного значення потенційної глибини V_0. Відповідно до результатів ми помітили, що деякі системи досягли гарної відповідності між теоретичними розрахунками та експериментальними даними квазіпружного розсіювання ($d\sigma qel$)/$d\sigma R$) і розрахунками розподілу при стандартному значенні глибини потенціалу або при значенні нижче ніж стандартне значення, і не було досягнуто відповідності при значенні, більшому за стандартне значення потенційної глибини V_0. Зроблено висновок, що значення величин квазіпружного розсіювання зростають при зменшенні величини потенціальної глибини.

Ключові слова: *квазіпружне розсіювання; потенціал Вудса-Саксона (WS); спарювання; система важких іонів; параметр дифузності поверхні*